

# One-dimensional arrangements of metal atoms in transition metal carbonyl complexes of mixed main group metal alkoxides

Michael Veith, Stefan Weidner, Klaus Kunze, Dieter Käfer, Johannes Hans and Volker Huch

*Institute for Inorganic Chemistry, University of the Saarland, Postfach 15 11 50, D-66041 Saarbrücken (Germany)*

(Received 30 October 1993; accepted 15 December 1993)

## CONTENTS

Abstract	297
1. Introduction	298
2. Syntheses of mixed metal alkoxide carbonyl complexes	298
2.1. Mixed main group metal alkoxides with $ns^2$ -configured elements	298
2.2. Synthesis of transition metal carbonyl complexes	301
2.3. Reactivity of $ns^2$ -configured main group elements towards transition metals	302
3. Structures, spectroscopy and bonding	307
3.1. Structural characterization of $ns^2$ -configured main group metal alkoxide transition metal carbonyl complexes	307
3.2. IR frequencies of CO in metal carbonyl complexes of mixed metal alkoxides	314
3.3. Some comments on a cluster concept	317
4. Oligomers and polymers with one-dimensionally arranged metal atoms	318
Acknowledgements	321
References	321

## ABSTRACT

Mixed metal alkoxides containing main group elements with  $ns^2$  electron configurations of the general formula  $M(O^tBu)_3M'$  ( $M = In, Tl$ ;  $M' = Ge, Sn, Pb$ ),  $M'(O^tBu)_3M(O^tBu)_3M'$  ( $M =$  divalent metal atom,  $M' = Ge, Sn$ ) and  $(O^tBu)M'(O^tBu)_2M(O^tBu)_2M(O^tBu)_2M'(O^tBu)$  ( $M = Co, Ni$ ;  $M' = Ge, Sn$ ) can be reacted with simple metal carbonyls. The products obtained are composed of a one-dimensional array of metal atoms held together by direct metal–metal bonds or by bridging alkoxide groups. The following compounds have been isolated and characterized by IR and NMR spectroscopy and X-ray diffraction ( $M' = Ge, Sn, Pb$ ;  $M = In, Tl$ ;  $M^T =$  transition metal):  $M'(O^tBu)_3M-M^T(CO)_n$ ,  $(CO)_nM^T-M(O^tBu)_3M'-M^T(CO)_n$ ,  $M'(O^tBu)_3M-M^T(CO)_nM(O^tBu)_3M'$ ,  $(CO)_nM^T-M'(O^tBu)_3M(O^tBu)_3M'-M^T(CO)_n$ ,  $(CO)_nM^T-M'[O^tBu](O^tBu)_2M(O^tBu)_2M(O^tBu)_2[O^tBu]M'-M^T(CO)_n$  and  $(CO)_nM^T-M'(O^tBu)_3M-M^T(CO)_nM(O^tBu)_3M'-M^T(CO)_n$ . In addition, an oligomeric species of the general formula  $[Sn(O^tBu)_3In-Mo(CO)_4]_n-Sn(O^tBu)_3In-Mo(CO)_5$  with  $n \approx 9, 10$  has been isolated.

*Correspondence to:* M. Veith, Institute for Inorganic Chemistry, University of the Saarland, Postfach 15 11 50, D-66041 Saarbrücken, Germany.

## 1. INTRODUCTION

It is well known that the transition metals may be coordinated by a wide variety of different ligands, most of which acting generally as electron donors. Classical  $\sigma$ -donor ligands such as  $\text{NH}_3$  and  $\text{OH}_2$  or  $\sigma$ -donors and  $\pi$ -acceptors such as  $\text{CO}$  and  $\text{PR}_3$  contain non-metallic elements which possess electron lone pairs and act as coordination centres to the transition metals. Another large group of ligands can be classified as  $\pi$ -systems, in which various atoms take part in bonding to the transition metal at the same time through the  $\pi$  ligand orbitals ( $\pi$ -complex). In addition to these classical ligands there is a comparatively small number of systems known in which a central metallic element acts as an electron donor. Most of these metals are main group elements in a low oxidation state, in particular the  $ns^2$  electron configuration, e.g.  $\text{Ge(II)}$  and  $\text{Sn(II)}$  [1].

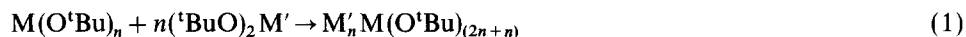
Some years ago we reported the synthesis of metal alkoxides which combine one or two main group metals in the  $ns^2$  configuration [2–4]. Compounds of type  $\text{M}(\text{O}^t\text{Bu})_3\text{M}'$  [ $\text{M} = \text{In(I)}, \text{Tl(I)}, \text{M}' = \text{Ge(II)}, \text{Sn(II)}, \text{Pb(II)}$ ] and  $\text{M}'(\text{O}^t\text{Bu})_3\text{M}(\text{O}^t\text{Bu})_3\text{M}'$  [ $\text{M} = \text{divalent metal cation}, \text{M}' = \text{Ge(II)}, \text{Sn(II)}, \text{Pb(II)}$ ] are of special interest, as they display two low-valent metallic elements which are situated on the axial sites of one or two (fused) trigonal bipyramids, thus making them accessible for complexation with transition metal carbonyls. This synthetic procedure should allow the construction of molecules with one-dimensionally arranged metallic elements. As will be discussed below, this can indeed be accomplished, and we have denoted these alkoxide compounds in view of their special structure and reactivity as “Janus-Head” molecules [5].

This review summarizes the mixed metal alkoxide–transition metal carbonyl complexes synthesized so far in our laboratory. Special consideration will be given to the structural properties of these compounds. A comparative study provides insight into the reactivity of low-valent elements in the  $ns^2$  electron configuration.

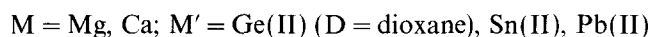
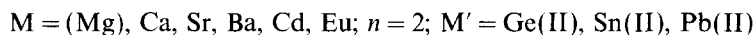
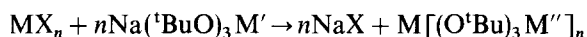
## 2. SYNTHESIS OF MIXED METAL ALKOXIDE CARBONYL COMPLEXES

2.1. Mixed metal alkoxides with  $ns^2$ -configured elements

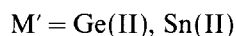
Mixed metal alkoxides of different metallic elements can be prepared by well established routes [6–8]. For alkoxides containing elements in the  $ns^2$  configuration, and with *tert*-butyl as the organic group, the following procedures [eqns. (1)–(3)] have been found to provide good yields.



$\text{M} = \text{Tl(I)}; n = 1; \text{M}' = \text{Ge(II)}, \text{Sn(II)}$

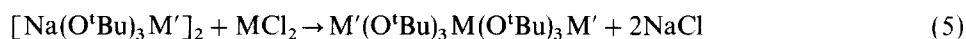


All reactions are performed in non-coordinating solvents and the yields of the products are 70–95%. The products are purified by sublimation or crystallization; however the choice of the reaction procedure may influence the yield [9]. In the  $\text{M}(\text{O}'\text{Bu})_3\text{M}'$  series, the synthesis of  $\text{Tl}(\text{O}'\text{Bu})_3\text{Sn}$  [10] and  $\text{In}(\text{O}'\text{Bu})_3\text{Sn}$  [11] have been described earlier. By similar routes,  $\text{Tl}(\text{O}'\text{Bu})_3\text{Ge}$ ,  $\text{Tl}(\text{O}'\text{Bu})_3\text{Pb}$  and  $\text{In}(\text{O}'\text{Bu})_3\text{Ge}$  have been obtained and characterized completely, and selected data are given in Table 1. As an alternative to  $[\text{Na}(\text{O}'\text{Bu})_3\text{M}']_2$  [12],  $\text{Tl}(\text{O}'\text{Bu})_3\text{M}'$  may be used by reaction with  $\text{InBr}$ , as shown in eqn. (4).



So far we have been unsuccessful in synthesizing  $\text{In}(\text{O}'\text{Bu})_3\text{Pb}$  by any of the routes described above.

Transition metals with a 3d configuration can be combined with  $\text{Ge(II)}$ ,  $\text{Sn(II)}$  and  $\text{Pb(II)}$  using *tert*-butoxy groups as bridging ligands. If sodium tris(*tert*-butoxy)germate or -plumbate is allowed to react with chlorides of  $\text{Cr}$ ,  $\text{Mn}$  or  $\text{Zn}$ , compounds of the type  $\text{M}'(\text{O}'\text{Bu})_3\text{M}(\text{O}'\text{Bu})_3\text{M}'$  are formed [eqn. (5)] [13].



On the other hand, if sodium tris(*tert*-butoxy)stannate, -germate or -plumbate is reacted with the chlorides of the smaller sized 3d elements, a new type of compound can be isolated from the reaction mixture, which has the general formula  $(\text{tBuO})\text{M}'(\text{O}'\text{Bu})_2\text{M}(\text{O}'\text{Bu})_2\text{M}(\text{O}'\text{Bu})_2\text{M}'(\text{O}'\text{Bu})$  and which combines two main group and two transition metals [eqn. (6)] [13].

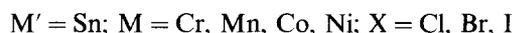
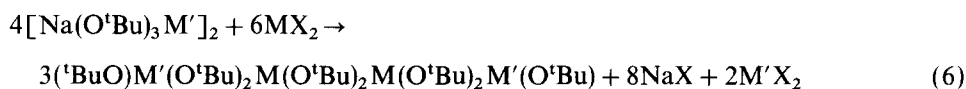


TABLE 1

Some data for compounds of the general formula  $M(O^tBu)_3M'$ 

Compound	Space group and lattice constants	$^1H$ NMR ( $\delta$ ppm)	Melting point/ $^{\circ}C$	Synthesis
$In(O^tBu)_3Ge^a$	<i>Pnma</i> $a = 12.53(1)$ $b = 15.51(2)$ $c = 9.604(8)$ $Z = 4$	1.39	52–54	(a) $Tl(O^tBu)_3Ge + InBr$ , yield 77.4% (b) $[Na(O^tBu)_3Ge]_2 + InBr$ , yield 71.8%
$In(O^tBu)_3Sn$ [10]	<i>P6<sub>3</sub>/m</i> $a = b = 9.867(9)$ $c = 11.21(1)$ $Z = 2$	1.37	41	(a) $Tl(O^tBu)_3Sn + InBr$ , yield 92% (b) $[Na(O^tBu)_3Sn]_2 + InBr$ , yield 90%
$Tl(O^tBu)_3Ge^a$	<i>Pnma</i> $a = 12.361(9)$ $b = 15.64(1)$ $c = 9.604(7)$ $Z = 4$	1.38	87–88	$[Tl(O^tBu)]_4 + [Ge(O^tBu)_2]_2$ , yield 92.9%
$Tl(O^tBu)_3Sn$ [9]	<i>P6<sub>3</sub>/m</i> $a = b = 9.944(5)$ $c = 11.07(1)$ $Z = 2$	1.32	43	$[Tl(O^tBu)]_4 + [Ge(O^tBu)_2]_2$ , yield 90%
$Tl(O^tBu)_3Pb^a$	<i>P6<sub>3</sub>/m</i> $a = b = 9.94(5)$ $c = 10.80(9)$ $Z = 2$	1.31	73–74	$[Tl(O^tBu)]_4 + [Pb(O^tBu)_2]_3$ , yield 71.7%

<sup>a</sup>Analytical data: for  $In(O^tBu)_3Ge$ , calc. C 35.44, H 6.69, found C 35.35, H 6.72%; for  $Tl(O^tBu)_3Ge$ , calc. C 29.04, H 5.48, found C 29.11, H 5.58%; and for  $Tl(O^tBu)_3Pb$ , calc. C 22.85, H 4.31, found C 22.70, H 4.34%.

$M' = Pb$ ;  $M = Co$ ;  $X = Cl$

In these compounds the transition metal is in a fourfold coordination site which can be described as a spiro metallic centre in a distorted oxygen tetrahedron [13].

An example of each of the different mixed metal alkoxides that have been used in the preparation of metal carbonyl complexes is shown in Fig. 1. The  $M(O^tBu)_3M'$  structure is the simplest, with a central  $MO_3M'$  core that can be described as a distorted trigonal bipyramid with the three oxygen atoms assembled in the equatorial plane and the two metallic elements in the apical positions.  $M'(O^tBu)_3M(O^tBu)_3M'$  can be formally viewed as two trigonal bipyramids fused together at the common divalent metallic element, which can either be a main group, a transition or a lanthanide (e.g. Eu) element. The  $(^tBuO)M'(O^tBu)_2M(O^tBu)_2M(O^tBu)_2M'(O^tBu)$  compounds have four metallic elements which are linked together by  $^tBuO$  bridges,

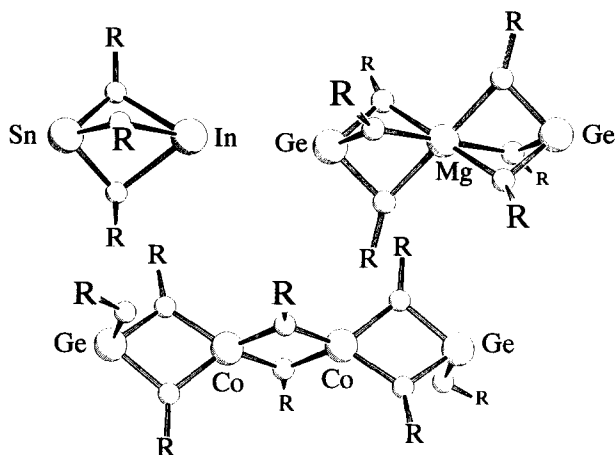
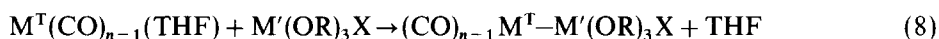
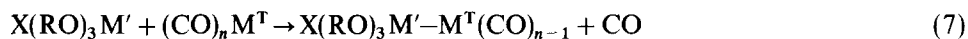


Fig. 1. Skeleton structure of three different mixed metal alkoxides:  $\text{Sn}(\text{OtBu})_3\text{In}$  [11],  $\text{Ge}(\text{OtBu})_3\text{Mg}(\text{OtBu})_3\text{Ge}$  [9] and  $(\text{BuO})\text{Ge}(\text{OtBu})_2\text{Co}(\text{OtBu})_2\text{Co}(\text{OtBu})_2\text{Ge}(\text{OtBu})$  [13] ( $\text{R} = \text{tert-Butyl}$ ; the non-designated balls represent oxygen atoms).

and three four-membered rings are arranged in a perpendicular fashion. The atoms  $\text{M}$  are in a distorted tetrahedral environment whereas the  $\text{M}'$  atoms are in a trigonal pyramidal coordination. Each end of the compound ( $\text{M}'$ ) is terminated by a *tert*-butoxy group and the oxygen atom is only dicoordinate.

## 2.2. Syntheses of transition metal carbonyl complexes

The formation of an  $\text{M}^{\text{T}}-\text{M}'$  bond ( $\text{M}^{\text{T}} = \text{transition metal}$ ,  $\text{M}' = ns^2 \text{ element}$ ) can be accomplished by two different procedures which are outlined in eqns. (7) and (8).



Reaction (7) may be described as a thermally induced CO substitution by a metal base. In contrast, reaction (8) relies on the photochemical formation of a labile THF complex which undergoes subsequent thermal reaction to lose the THF ligand, allowing for complexation of the  $ns^2$ -metal centre. These well known reactions have been widely used in transition metal chemistry [14,15] have been transferred to alkoxides of simple  $ns^2$  elements some time ago [16–18]. When two ligand sites at a transition metal have to be displaced simultaneously, the norbornadiene (nbd)

route has proved very successful [19] and has been adopted for  $ns^2$ -metal alkoxides [eqn. (9)].



Table 2 lists the mixed metal alkoxide transition metal carbonyl complexes, together with the synthetic procedure used and the experimental conditions. The isolated yields of the products can attain 95%. The compounds are abbreviated with the first letters of the metallic elements. Thus **TSM** designates the compound  $Tl(O^tBu)_3SnMo(CO)_5$  and **CSESC** the compound  $(CO)_5CrSn(OtBu)_3Eu(OtBu)_3SnCr(CO)_5$ ; the number of letters is equal to the number of metallic elements present in the compound. In some instances different elements are designated by the same letter (e.g. Sn and Sr), but it is clear from the order of the letters (which is strictly structural) that **FSSSF** denotes the compound  $(CO)_4Fe-Sn(O^tBu)_3Sr(O^tBu)_3SnFe(CO)_4$  and the middle S refers to strontium (with respect to the alkoxides used another interpretation would not make sense).

The easiest bonding formation  $M'-M^T$  ( $M'$  = metal with  $ns^2$  configuration,  $M^T$  = transition metal) is accomplished using the method depicted in eqn. (8), which can be performed under mild conditions (see Table 2). The thermal carbonyl displacement method [eqn. (7)] may require high temperatures and long reaction times when carbonyls of Cr, Mo or W are used. The norbornadiene displacement [eqn. (9)] requires higher temperatures and longer heating than the THF displacement. This difference can be attributed to the fact that the norbornadiene is more strongly bound than THF to the transition metal [19].

As indicated in Table 2, the products of reactions (7)–(9) may be isolated by either crystallization or sublimation. All products are solids at ordinary temperatures. They can be readily characterized by  $^1H$  NMR and IR spectroscopy (Table 3). The latter method not only gives some insight into the bonding of the CO groups [20,21], but can also be used to distinguish between cis and trans arrangements in compounds of the type  $M'(O^tBu)_3In-M^T(CO)_4-In(O^tBu)_3M'$ , which have a local symmetry of either  $C_{2v}$  or  $D_{4h}$  at the transition metal,  $M^T$  [22,23]. Table 3 lists only  $A_1$  stretching frequencies, which are assigned to the carbonyl group situated trans to the  $M'-M^T$  bond [24].

### 2.3. Reactivity of $ns^2$ -configured main group elements towards transition metals

Comparison of the reaction times and temperatures in Table 2 reveals distinct differences in the thermal reaction of metal carbonyls with metal alkoxides. If the  $ns^2$  element is constant the reactivity trend  $Ni(CO)_4 > Fe_2(CO)_9 > Mo(CO)_6 > Cr(CO)_6 > W(CO)_6$  can be established and is consistent with established results of other substitution reactions [20]. On the other hand, there is also a pronounced

TABLE 2

Synthetic procedures for mixed main group metal alkoxide transition metal carbonyl complexes (R = *tert*-butyl)

Compound and abbreviations	Conditions and yield <sup>a</sup>
Tl(OR) <sub>3</sub> Sn–Cr(CO) <sub>5</sub> ( <b>TSC</b> )	(OC) <sub>5</sub> Cr*THF/THF/RT/12 h/S/50%
Tl(OR) <sub>3</sub> Sn–Mo(CO) <sub>5</sub> ( <b>TSM</b> )	Mo(CO) <sub>6</sub> /T/105°C/5 h/S/70%
Tl(OR) <sub>3</sub> Sn–W(CO) <sub>5</sub> ( <b>TSW</b> )	(OC) <sub>5</sub> W*THF/THF/RT/12 h/S/47%
Sn(OR) <sub>3</sub> In–Cr(CO) <sub>5</sub> ( <b>SIC</b> )	Cr(CO) <sub>6</sub> /T/110°C/40 h/S/35%
Sn(OR) <sub>3</sub> In–Mo(CO) <sub>5</sub> ( <b>SIM</b> )	Mo(CO) <sub>6</sub> /T/80°C/5 h/S/39%
Sn(OR) <sub>3</sub> In–W(CO) <sub>5</sub> ( <b>SIW</b> )	W(CO) <sub>6</sub> /T/95°C/2 d/S/17%
Sn(OR) <sub>3</sub> In–Fe(CO) <sub>4</sub> ( <b>SIF</b> )	Fe <sub>2</sub> (CO) <sub>9</sub> /T/RT/3 h/–/quant.
Ge(OR) <sub>3</sub> In–Cr(CO) <sub>5</sub> ( <b>GIC</b> )	Cr(CO) <sub>6</sub> /T/85°C/13 h/S/41%
Ge(OR) <sub>3</sub> In–Mo(CO) <sub>5</sub> ( <b>GIM</b> )	Mo(CO) <sub>6</sub> /T/80°C/3 h/S/45%
Ge(OR) <sub>3</sub> In–W(CO) <sub>5</sub> ( <b>GIW</b> )	W(CO) <sub>6</sub> /T/90°C/1 d/–/n.d.
(OC) <sub>5</sub> Cr–In(OR) <sub>3</sub> Sn–Cr(CO) <sub>5</sub> ( <b>CISC</b> )	( <b>SIC</b> ) + (OC) <sub>5</sub> Cr*THF/THF/RT/24 h/C/80%
(OC) <sub>5</sub> Mo–In(OR) <sub>3</sub> Sn–Mo(CO) <sub>5</sub> ( <b>MISM</b> )	2Mo(CO) <sub>6</sub> /T/80°C/11 h/C/83%
(OC) <sub>5</sub> Mo–In(OR) <sub>3</sub> Sn–Cr(CO) <sub>5</sub> ( <b>MISC</b> )	( <b>SIM</b> ) + (OC) <sub>5</sub> Cr*THF/THF/RT/24 h/C/75%
(OC) <sub>5</sub> Cr–In(OR) <sub>3</sub> Sn–Mo(CO) <sub>5</sub> ( <b>CISM</b> )	( <b>SIC</b> ) + (OC) <sub>5</sub> Mo*THF/THF/RT/24 h/C/58%
(OC) <sub>5</sub> Fe–In(OR) <sub>2</sub> Sn–Cr(CO) <sub>5</sub> ( <b>FISC</b> )	( <b>SIF</b> ) + (OC) <sub>5</sub> Cr*THF/THF/RT/24 h/C/45%
(OC) <sub>3</sub> Ni–In(OR) <sub>3</sub> Sn–Ni(CO) <sub>3</sub> ( <b>NISN</b> )	2Ni(CO) <sub>4</sub> /T/RT/1 h/C/n.d.
(OC) <sub>5</sub> Cr–In(OR) <sub>3</sub> Ge–Cr(CO) <sub>5</sub> ( <b>CIGC</b> )	2Cr(CO) <sub>6</sub> /T/90°C/56 h/C/n.d.
(OC) <sub>5</sub> Mo–In(OR) <sub>3</sub> Ge–Mo(CO) <sub>5</sub> ( <b>MIGM</b> )	2Cr(CO) <sub>6</sub> /T/80°C/8 h/C/75%
(OC) <sub>5</sub> Mo–In(OR) <sub>3</sub> Ge–Cr(CO) <sub>5</sub> ( <b>MIGC</b> )	( <b>GIM</b> ) + (OC) <sub>5</sub> Cr*THF/THF/RT/24 h/C/70%
(OC) <sub>5</sub> W–In(OR) <sub>3</sub> Ge–Cr(CO) <sub>5</sub> ( <b>WIGC</b> )	( <b>GIW</b> ) + Cr(OC) <sub>6</sub> /T/90°C/60 h/C/62%
(OC) <sub>4</sub> Fe–In(OR) <sub>3</sub> Ge–Fe(CO) <sub>4</sub> ( <b>FIGF</b> )	2Fe <sub>2</sub> (CO) <sub>9</sub> /T/RT/11 h/C/48%
(OC) <sub>5</sub> Mo–In(OR) <sub>3</sub> Ge–Fe(CO) <sub>4</sub> ( <b>MIGF</b> )	( <b>GIM</b> ) + Fe <sub>2</sub> (CO) <sub>9</sub> /T/RT/10 h/C/65%
(OC) <sub>3</sub> Ni–In(OR) <sub>3</sub> Ge–Ni(CO) <sub>3</sub> ( <b>NIGN</b> )	2Ni(CO) <sub>4</sub> /T/–20°C/1 h/C/70%
<i>trans</i> -[Tl(OR) <sub>3</sub> Sn] <sub>2</sub> Cr(CO) <sub>4</sub> ( <b>TSCST</b> )	nbd Cr(CO) <sub>4</sub> /BF/80°C/2 d/C/40%
<i>trans</i> -[Tl(OR) <sub>3</sub> Sn] <sub>2</sub> Mo(CO) <sub>4</sub> ( <b>TSMST</b> )	nbd Mo(CO) <sub>4</sub> /BF/70°C/1 d/C/73%
<i>cis</i> -[Sn(OR) <sub>3</sub> In] <sub>2</sub> Cr(CO) <sub>4</sub> ( <b>SICIS</b> )	nbd Cr(CO) <sub>4</sub> /BF/70°C/1 d/C/72%
[Sn(OR) <sub>3</sub> In] <sub>2</sub> Mo(CO) <sub>4</sub> ( <b>SIMIS</b> )	nbd Mo(CO) <sub>4</sub> /BF/65°C/1 d/C/84%
<i>cis</i> -[Sn(OR) <sub>3</sub> In] <sub>2</sub> W(CO) <sub>4</sub> ( <b>SIWIS</b> )	nbd W(CO) <sub>4</sub> /BF/80°C/2 d/C/75%
<i>cis</i> -[Ge(OR) <sub>3</sub> In] <sub>2</sub> Cr(CO) <sub>4</sub> ( <b>GICIG</b> )	nbd Cr(CO) <sub>4</sub> /BF/70°C/1 d/C/89%
<i>cis</i> -[(OC) <sub>5</sub> Cr–Sn(OR) <sub>3</sub> In] <sub>2</sub> Cr(CO) <sub>4</sub> ( <b>CSICISC</b> )	( <b>SICIS</b> ) + 2(OC) <sub>5</sub> Cr*THF/THF/RT/24 h/C/75%
[(OC) <sub>5</sub> Cr–Sn(OR) <sub>3</sub> In] <sub>2</sub> Mo(CO) <sub>4</sub> ( <b>CSMISC</b> )	( <b>SIMIS</b> ) + 2(OC) <sub>5</sub> Cr*THF/THF/RT/24 h/C/61%
(OC) <sub>4</sub> Fe–Sn(OR) <sub>3</sub> Sr(OR) <sub>3</sub> Sn–Fe(CO) <sub>4</sub> ( <b>FSSSF</b> )	2Fe <sub>2</sub> (CO) <sub>9</sub> /T/RT/20 h/C/36%
(OC) <sub>5</sub> Cr–Sn(OR) <sub>3</sub> Eu(OR) <sub>3</sub> Sn–Cr(CO) <sub>5</sub> ( <b>CSESC</b> )	2Cr(CO) <sub>6</sub> /B/80°C/5 h/C/48%
(OC) <sub>5</sub> Cr–Sn(OR) <sub>3</sub> Ba(OR) <sub>3</sub> Sn–Cr(CO) <sub>5</sub> ( <b>CSBSC</b> )	2Cr(CO) <sub>6</sub> /B/80°C/60 h/C/41%
(OC) <sub>5</sub> Cr–Sn(OR) <sub>3</sub> Sr(OR) <sub>3</sub> Sn–Cr(CO) <sub>5</sub> ( <b>CSSSC</b> )	2Cr(CO) <sub>6</sub> /T/100°C/17 h/D/88%

TABLE 2 (continued)

[Co(OR) <sub>4</sub> Sn–Fe(CO) <sub>4</sub> ] <sub>2</sub> ( <b>FSCCSF</b> )	2Fe <sub>2</sub> (CO) <sub>9</sub> /T/RT/18 h/C/44%
(OC) <sub>4</sub> Fe–Sn(OR) <sub>3</sub> Pb(OR) <sub>3</sub> Sn–Fe(CO) <sub>4</sub> ( <b>FSPSF</b> )	2Fe <sub>2</sub> (CO) <sub>9</sub> /T/RT/12 h/C/84%
[(RO) <sub>2</sub> GeORFe(CO) <sub>4</sub> ] <sub>2</sub> Pb ( <b>GFPFG</b> )	2Fe <sub>2</sub> (CO) <sub>9</sub> /T/RT/2 h/C/95%
[Na(O <sup>t</sup> Bu) <sub>3</sub> Ge–Ni(CO) <sub>3</sub> ] <sub>2</sub> ( <b>NGN</b> ) <sup>b</sup>	2Ni(CO) <sub>4</sub> /T/5°C/30 min/D/97%
[Na(O <sup>t</sup> Bu) <sub>3</sub> Sn–Ni(CO) <sub>3</sub> ] <sub>2</sub> ( <b>NSN</b> ) <sup>b</sup>	2Ni(CO) <sub>4</sub> /T/12°C/30 min/D/94%
[Na(O <sup>t</sup> Bu) <sub>3</sub> Ge–Mo(CO) <sub>5</sub> ] <sub>2</sub> ( <b>NGM</b> ) <sup>b</sup>	2Mo(CO) <sub>6</sub> /T/80°C/3 h/D/95%
[Na(O <sup>t</sup> Bu) <sub>3</sub> Sn–Mo(CO) <sub>5</sub> ] <sub>2</sub> ( <b>NSM</b> ) <sup>b</sup>	2Mo(CO) <sub>6</sub> /T/85°C/3 h/D/93%

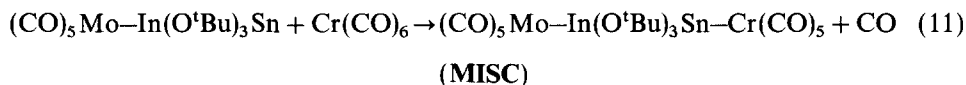
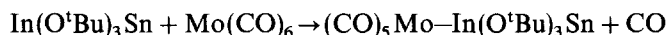
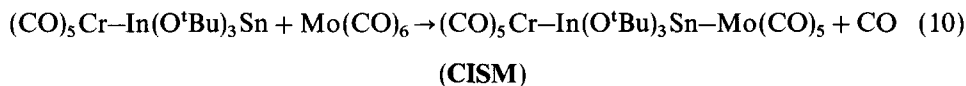
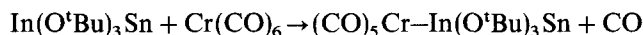
<sup>a</sup>The order of the information is as follows: starting compound with respect to metal carbonyl/solvent (B = benzene, T = toluene, BF = benzene-fraction (b.p. 100–140°C), THF = tetrahydrofuran)/reaction temperature (RT = room temperature)/reaction time/method of separation (C = crystallization, S = sublimation, D = deposition)/yield in % (n.d. = not determined).

<sup>b</sup>Data to be published elsewhere.

difference in reactivity at the *ns*<sup>2</sup> element and the following series has been assessed: In(I) >> Ge(II) > Sn(II) > Tl(I), Pb(II).

We have been unsuccessful in preparing Tl(I) or Pb(II) complexes of transition metals, although some complexes have been obtained with different ligands at these metal atoms [25,26]. For example, Tl(O<sup>t</sup>Bu)<sub>3</sub>Sn will exclusively react with Mo(CO)<sub>6</sub> to give Tl(O<sup>t</sup>Bu)<sub>3</sub>Sn–Mo(CO)<sub>5</sub>. No evidence of the substitution product formed by complexation at the thallium atom is obtained from the IR and NMR spectra of the reaction mixture. The Sn–Mo bond can be unambiguously established by an X-ray structure determination [11].

The indium(I) centre in the “Janus-Head” molecules of the type In(O<sup>t</sup>Bu)<sub>3</sub>M' (M' = Ge, Sn) is much more reactive than the germanium or tin centres. For example, the two isomers (CO)<sub>5</sub>Cr–In(O<sup>t</sup>Bu)<sub>3</sub>Sn–Mo(CO)<sub>5</sub> (**CISM**) and (CO)<sub>5</sub>Mo–In(O<sup>t</sup>Bu)<sub>3</sub>Sn–Cr(CO)<sub>5</sub> (**MISC**) can be synthesized separately as displayed in eqns. (10) and (11) and are found to have distinctly different physical properties and different IR data (see Table 3) [11].



The structures of **MISC** and **CISM** have been confirmed by X-ray crystallography, revealing structural differences. **CISM** crystallizes in the orthorhombic space group

TABLE 3

<sup>1</sup>H NMR (δ, ppm) and IR [CO stretch trans to M<sup>T</sup>–M bond or M(CO)<sub>n</sub> group in cm<sup>-1</sup>]

Compound and abbreviation	<sup>1</sup> H NMR	IR (KBr)		IR (solution)	
		Ge/ Sn–M <sup>T</sup>	Tl/ In–M <sup>T</sup>	Ge/ Sn–M <sup>T</sup>	Tl/ In–M <sup>T</sup>
Tl(OR) <sub>3</sub> Sn–Cr(CO) <sub>5</sub> ( <b>TSC</b> )	1.31			2060 (B)	
Tl(OR) <sub>3</sub> Sn–Mo(CO) <sub>5</sub> ( <b>TSM</b> )	1.31			2070 (B)	
Tl(OR) <sub>3</sub> Sn–W(CO) <sub>5</sub> ( <b>TSW</b> )	1.30			2060 (B)	
Sn(OR) <sub>3</sub> In–Cr(CO) <sub>5</sub> ( <b>SIC</b> )	1.23			(T)	2033
Sn(OR) <sub>3</sub> In–Mo(CO) <sub>5</sub> ( <b>SIM</b> )	1.23		2061	(T)	2051
Sn(OR) <sub>3</sub> In–W(CO) <sub>5</sub> ( <b>SIW</b> )	1.23		2052		
Sn(OR) <sub>3</sub> In–Fe(CO) <sub>4</sub> ( <b>SIF</b> )	1.21				
Ge(OR) <sub>3</sub> In–Cr(CO) <sub>5</sub> ( <b>GIC</b> )	1.26		2036		
Ge(OR) <sub>3</sub> In–Mo(CO) <sub>5</sub> ( <b>GIM</b> )	1.26		2064	(T)	2058
(OC) <sub>5</sub> Cr–In(OR) <sub>3</sub> Sn–Cr(CO) <sub>5</sub> ( <b>CISC</b> )	1.27			2058 (T)	2042
(OC) <sub>5</sub> Mo–In(OR) <sub>3</sub> Sn–Mo(CO) <sub>5</sub> ( <b>MISM</b> )	1.28	2071	2058	2069 (T)	2050
(OC) <sub>5</sub> Mo–In(OR) <sub>3</sub> Sn–Cr(CO) <sub>5</sub> ( <b>MISC</b> )	1.28			2059 (T)	2051
(OC) <sub>5</sub> Cr–In(OR) <sub>3</sub> Sn–Mo(CO) <sub>5</sub> ( <b>CISM</b> )	1.28			2069 (T)	2033
(OC) <sub>5</sub> Fe–In(OR) <sub>2</sub> Sn–Cr(CO) <sub>5</sub> ( <b>FISC</b> )	1.28			2061 (T)	2041
(OC) <sub>3</sub> Ni–In(OR) <sub>3</sub> Sn–Ni(CO) <sub>3</sub> ( <b>NISN</b> )	1.27				
(OC) <sub>5</sub> Mo–In(OR) <sub>3</sub> Ge–Mo(CO) <sub>5</sub> ( <b>MIGM</b> )	1.32	2076	2063		
(OC) <sub>5</sub> Mo–In(OR) <sub>3</sub> Ge–Cr(CO) <sub>5</sub> ( <b>MIGC</b> )	1.32			2068 (T)	2055
(OC) <sub>5</sub> W–In(OR) <sub>3</sub> Ge–Cr(CO) <sub>5</sub> ( <b>WIGC</b> )	1.31	2060	2051		
(OC) <sub>4</sub> Fe–In(OR) <sub>3</sub> Ge–Fe(CO) <sub>4</sub> ( <b>FIGF</b> )	1.31	2065	2046		
(OC) <sub>5</sub> Mo–In(OR) <sub>3</sub> Ge–Fe(CO) <sub>4</sub> ( <b>MIGF</b> )	1.32	2068	2055		
(OC) <sub>3</sub> Ni–In(OR) <sub>3</sub> Ge–Ni(CO) <sub>3</sub> ( <b>NIGN</b> )	1.31	2088	2069		
	<sup>1</sup> H NMR	IR (THF)			
				M(II)–M <sup>T</sup> (CO) <sub>4</sub> –M(II)	M(I)–M <sup>T</sup> (CO) <sub>4</sub> –M(I)
<i>trans</i> -[Tl(OR) <sub>3</sub> Sn] <sub>2</sub> Cr(CO) <sub>6</sub> ( <b>TSCST</b> )	1.51	1865 (E <sub>u</sub> )			
<i>trans</i> -[Tl(OR) <sub>3</sub> Sn] <sub>2</sub> Mo(CO) <sub>4</sub> ( <b>TSMST</b> )	1.50	1887 (E <sub>u</sub> )			

TABLE 3 (continued)

<i>cis</i> -[Sn(OR) <sub>3</sub> In] <sub>2</sub> Cr(CO) <sub>4</sub> ( <b>SICIS</b> )	1.43	1963 (A <sub>1</sub> <sup>1b</sup> )
[Sn(OR) <sub>3</sub> In] <sub>2</sub> Mo(CO) <sub>4</sub> ( <b>SIMIS</b> )	1.42	1987 (A <sub>1</sub> <sup>1b</sup> )
	1.44	
<i>cis</i> -[Sn(OR) <sub>3</sub> In] <sub>2</sub> W(CO) <sub>4</sub> ( <b>SIWIS</b> )	1.43	1982 (A <sub>1</sub> <sup>1b</sup> )
<i>cis</i> -[Ge(OR) <sub>2</sub> In] <sub>2</sub> Cr(CO) <sub>4</sub> ( <b>GICIG</b> )	1.43	1969 (A <sub>1</sub> <sup>1b</sup> )
	<sup>1</sup> H NMR	IR (THF)
		M(II)–M <sup>T</sup> (CO) <sub>n</sub> (A <sub>1</sub> <sup>1b</sup> )
(OC) <sub>4</sub> Fe–Sn(OR) <sub>3</sub> Sr(OR) <sub>3</sub> Sn–Fe(CO) <sub>4</sub> ( <b>FSSSF</b> )	1.40	2040 (N)
(OC) <sub>5</sub> Cr–Sn(OR) <sub>3</sub> Eu(OR) <sub>3</sub> Sn–Cr(CO) <sub>5</sub> ( <b>CSESC</b> )		2060 (N)
(OC) <sub>5</sub> Cr–Sn(OR) <sub>3</sub> Ba(OR) <sub>3</sub> Sn–Cr(CO) <sub>5</sub> ( <b>CSBSC</b> )	1.36	
(OC) <sub>5</sub> Cr–Sn(OR) <sub>3</sub> Sr(OR) <sub>3</sub> Sn–Cr(CO) <sub>5</sub> ( <b>CSSSC</b> )		2060 (N)
(OC) <sub>5</sub> Mo–Sn(OR) <sub>3</sub> Sr(OR) <sub>3</sub> Sn–Mo(CO) <sub>5</sub> ( <b>MSSSM</b> )		2070 (N)
[Co(OR) <sub>4</sub> Sn–Fe(CO) <sub>4</sub> ] <sub>2</sub> ( <b>CSFSC</b> )		2040 (N)
(OC) <sub>4</sub> Fe–Sn(OR) <sub>3</sub> Pb(OR) <sub>3</sub> Sn–Fe(CO) <sub>4</sub> ( <b>FSPSF</b> )	1.42	2040 (T)
	IR (KBr)	
		M(II)–M <sup>T</sup> (CO) <sub>n</sub> (A <sub>1</sub> <sup>1b</sup> )
Na(O <sup>t</sup> Bu) <sub>3</sub> Ge–Ni(CO) <sub>3</sub> ] <sub>2</sub> ( <b>NGN</b> )	2054 <sup>b</sup>	
Na(O <sup>t</sup> Bu) <sub>3</sub> Sn–Ni(CO) <sub>3</sub> ] <sub>2</sub> ( <b>NSN</b> )	2056 <sup>b</sup>	
Na(O <sup>t</sup> Bu) <sub>3</sub> Ge–Mo(CO) <sub>5</sub> ] <sub>2</sub> ( <b>NGM</b> )	2067 <sup>b</sup>	
Na(O <sup>t</sup> Bu) <sub>3</sub> Sn–Mo(CO) <sub>5</sub> ] <sub>2</sub> ( <b>NSM</b> )	2065 <sup>b</sup>	

<sup>a</sup>B = benzene; N = nujol; T = toluene; THF = tetrahydrofuran; R = *tert*-butyl.

<sup>b</sup>Data to be published elsewhere.

*Pnma* [*a* = 14.93(2), *b* = 14.33(2), *c* = 15.46(2), *Z* = 4] and **MISC** in the monoclinic space group *P2*<sub>1</sub>/*n* [*a* = 10.51(1), *b* = 30.30(2), *c* = 10.748(7), β = 107.36(7)°, *Z* = 4] [11].

The indium atom is more reactive towards metal carbonyls than germanium or tin in In(O<sup>t</sup>Bu)<sub>3</sub>M'. This may be explained by the fact that the <sup>t</sup>BuO group has a formal charge of –1, and the two metals have charges In +1 and Ge/Sn +2. The indium atom should therefore be more basic than germanium or tin. Conversely, elements within the Periodic Table tend to become less basic with increasing atomic mass, which is often explained by a more diffuse character of the orbitals of heavy main group elements [27]. Hence In(I) should be less basic than Ge(II). From our

experimental results, it seems that the charge effect is more important than the size effect.

### 3. STRUCTURES, SPECTROSCOPY AND BONDING

#### 3.1. Structural characterization of $ns^2$ -configured main group metal alkoxide transition metal carbonyl complexes

A number of metal carbonyl complexes of mixed metal alkoxides have been characterized by X-ray crystallography. Table 4 lists crystal data not available elsewhere [28]. Table 5 lists selected molecular distances [28] together with those of the non-complexed alkoxides  $\text{In}(\text{O}^t\text{Bu})_3\text{Sn}$  (**IS**),  $\text{Tl}(\text{O}^t\text{Bu})_3\text{Sn}$  (**TS**),  $\text{Sn}(\text{O}^t\text{Bu})_3$   $\text{Pb}(\text{O}^t\text{Bu})_3\text{Sn}$  (**SPS**) and  $\text{Ge}(\text{O}^t\text{Bu})_3\text{Ca}(\text{O}^t\text{Bu})_3\text{Ge}$  (**GCG**). In Fig. 2 the data for the complexes have been arranged in a diagram with increasing  $\text{M}' \cdots \text{M}$  distance. Drawings of the molecular structures are displayed in Figs. 3–9. The labelling of carbon atoms and carbonyl oxygen atoms has been omitted for clarity.

As can be seen from the figures, all metallic elements in the molecules are arranged in one-dimensional chains, with some of the metal atoms displaying direct metal–metal bonding. Apart from the direct metal–metal bonds, some of the metals are held close together by three oxygen bridges which are disposed outside the metal chain and which originate from the coordination of the alkoxide groups. Whereas in most of the compounds the one-dimensional array of metal atoms is linear, some compounds show a bend angle of  $96$ – $99^\circ$  at the central transition metal [**GICIG**,  $95.8(1)^\circ$ ; **CSICISC**,  $98.6(3)^\circ$ , **CSIMISC**,  $97.9(3)^\circ$ ]. This is due to the fact that bis-substitution at the central pseudo-octahedral transition metal is in cis positions. As we have noted before [29], the distortion from linearity in **FSPSF** (in a simplified model) is due to the central metallic element Pb, which has a  $6s^2$  configuration (stereochemical activity of the lone pair).

The reason for the difference in structure between the bent cis-compound **GICIG** and the linear trans-compound **TSMST** is unclear. As the trigonal pyramidally coordinated  $ns^2$  elements are poorer  $\pi$ -acceptors than carbon monoxide, the substitution of a second ligand should occur in a cis position [30–33]. On the other hand, steric requirements also play an important part in ligand distributions around a metallic element and, owing to the bulkiness of the “Janus-Head” molecules, a trans arrangement should be favoured. Examination of *trans*-**TSMST** and *cis*-**GICIG**, **-CSICISC** and **-CSIMISC** reveals that the cone angle  $\text{O}-\text{M}'-\text{O}$  at the main group element bound to the transition metal and the  $\text{M}'-\text{O}$  distance are different. For **TSMST** the mean  $\text{O}-\text{Sn}-\text{O}$  angle =  $84.3^\circ$  [ $\text{Sn}-\text{O} = 2.04(3) \text{ \AA}$ ] whereas for **GICIG**  $\text{O}-\text{In}-\text{O} = 66.3^\circ$  [ $\text{In}-\text{O} = 2.24(1) \text{ \AA}$ ], for **CSICISC**  $\text{O}-\text{In}-\text{O} = 68.5^\circ$  [ $\text{In}-\text{O} = 2.26(2) \text{ \AA}$ ] and for **CSIMISC**  $\text{O}-\text{In}-\text{O} = 67.7^\circ$  [ $\text{In}-\text{O} = 2.27(2) \text{ \AA}$ ]. Therefore, the indium atom can be characterized as much softer and more flexible for geometrical constraints compared with tin, a classification we have already found by comparing

TABLE 4

Crystal data for some new metal carbonyl complexes of mixed metal alkoxides [28]

Compound	Crystal system	Space group	Lattice constants Å, °	Molecules per unit (Z)	R (R <sub>w</sub> ) <sup>b</sup>	Symmetry
C <sub>21</sub> H <sub>27</sub> CrFeInO <sub>12</sub> Sn (FISC)	Monoclinic	P2 <sub>1</sub> /n	a 12.122(9) b 18.646(19) c 13.666(9) β 92.07(8)	4	0.0776 (0.0678)	C <sub>1</sub>
C <sub>22</sub> H <sub>27</sub> GeInMo <sub>2</sub> O <sub>13</sub> (MIGM)	Monoclinic	P2 <sub>1</sub> /n	a 10.470(9) b 30.40(2) c 10.720(9) β 107.36(8)	4	0.0707 (0.0704)	C <sub>1</sub>
C <sub>28</sub> H <sub>54</sub> CrGe <sub>2</sub> In <sub>2</sub> O <sub>10</sub> (GICIG)	Monoclinic	P2 <sub>1</sub> /n	a 10.137(8) b 26.30(2) c 16.030(9) β 91.22(2)	4	0.0637 (0.0632)	C <sub>1</sub>
C <sub>28</sub> H <sub>54</sub> MoO <sub>10</sub> Sn <sub>2</sub> Tl <sub>2</sub> (TSMST) <sup>a</sup>	Tetragonal	P4 <sub>2</sub> /n	a 20.65(2) c 10.029(8)	4	0.1273	C <sub>i</sub>
C <sub>32</sub> H <sub>54</sub> Fe <sub>2</sub> O <sub>14</sub> Sn <sub>2</sub> Sr (FSSSF)	Monoclinic	P2 <sub>1</sub> /n	a 10.598(5) b 13.681(8) c 15.982(8) β 97.06(4)	2	0.0507 (0.0476)	C <sub>i</sub>
C <sub>34</sub> H <sub>54</sub> BaCr <sub>2</sub> O <sub>16</sub> Sn <sub>2</sub> (CSBSC)	Monoclinic	P2 <sub>1</sub> /n	a 15.408(9) b 10.014(8) c 15.799(9) β 98.39(5)	2	0.0463 (0.0460)	C <sub>i</sub>
C <sub>38</sub> H <sub>54</sub> Cr <sub>3</sub> In <sub>2</sub> O <sub>20</sub> Sn <sub>2</sub> (CSICISC)	Triclinic	P $\bar{1}$	a 13.714(9) b 16.102(13) c 16.244(9) α 114.43(7) β 112.87(6) γ 97.12(7)	2	0.0796 (0.0763)	C <sub>1</sub>
C <sub>38</sub> H <sub>54</sub> Cr <sub>2</sub> In <sub>2</sub> MoO <sub>20</sub> Sn <sub>2</sub> (CSIMISC) <sup>a</sup>	Triclinic	P $\bar{1}$	a 13.78(2) b 16.13(4) c 16.29(4) α 114.0(1) β 112.6(1) γ 97.6(1)	2	0.0973 (0.0954)	C <sub>1</sub>

<sup>a</sup>Bad crystalline material: crystals of TSMST might be twinned.<sup>b</sup>R value (R<sub>w</sub> = weighted R) of structure refinement.

TABLE 5

The most pertinent molecular dimensions (Å) in some metal carbonyl complexes of mixed metal alkoxides [28]

Compound	M···M	In–M(T)	Ge/Sn–M(T)	M–O	Ge/Sn–O
<b>MIGM</b>	2.954(2)	2.702(4)	2.567(4)	2.244(9)	1.842(9)
<b>GICIG</b>	2.962(2)	2.563(4)	—	2.236(9)	1.872(8)
<b>FISC</b>	3.046(1)	2.420(9)	2.574(9)	2.187(20)	2.034(20)
<b>MISM</b> [11]	3.078(1)	2.742(1)	2.761(1)	2.141(6)	2.122(9)
<b>MISC</b> [11]	3.087(2)	2.734(2)	2.636(3)	2.213(9)	2.067(9)
<b>CSICISC</b>	3.116(2)	2.571(3)	2.596(6)	2.263(15)	2.025(12)
<b>CSIMISC</b>	3.123(3)	2.710(5)	2.592(6)	2.271(17)	2.003(13)
<b>FSSSF</b>	3.292(1)	—	2.491(2)	2.550(6)	2.027(6)
<b>TSM</b> [11]	3.298(1)	—	2.770(2)	2.557(15)	2.017(9)
<b>TSMST</b>	3.320(3)	—	2.687(5)	2.568(50)	2.036(30)
<b>FSPSF</b> [29]	3.327(1)	—	2.476(1)	2.593(20)	2.016(9)
<b>CSBSC</b>	3.493(1)	—	2.649(3)	2.705(6)	2.034(5)
<b>IS</b> [11]	3.200(3)	—	—	2.413(4)	2.032(4)
<b>TS</b> [10]	3.306(3)	—	—	2.595(7)	2.023(9)
<b>SPS</b> [9]	3.361(1)	—	—	2.56(2)	2.074(8)
<b>GCG</b> <sup>a</sup> [9]	2.999(2)	—	—	2.36(1)	1.903(3)

<sup>a</sup>Ge(O<sup>t</sup>Bu)<sub>3</sub>Ca(O<sup>t</sup>Bu)<sub>3</sub>Ge as reference for a normal Ge–O bond length.

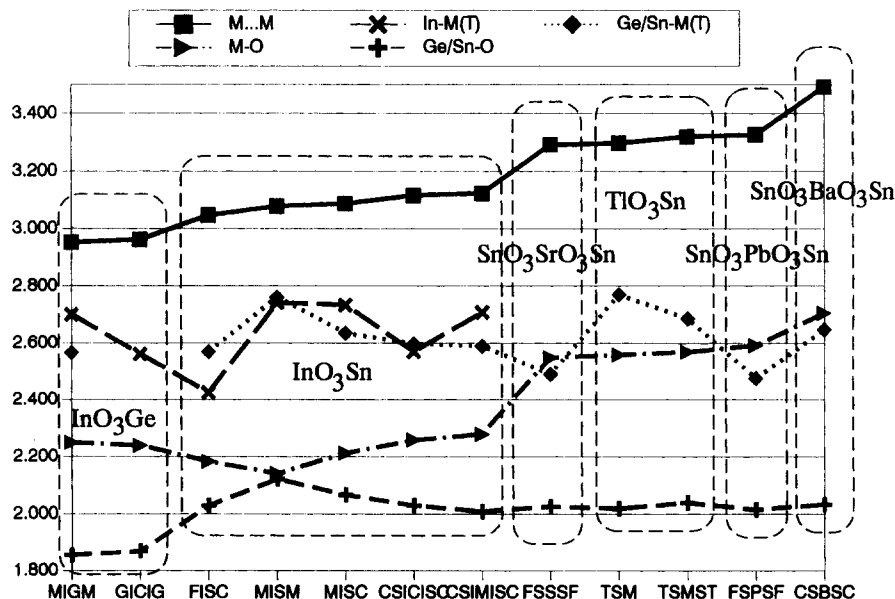


Fig. 2. Plot of different distances (in Å) within metal alkoxide metal carbonyl complexes. The inner skeleton formulae of the alkoxides are used to separate different groups of compounds. For the designation of the compounds, see the text.

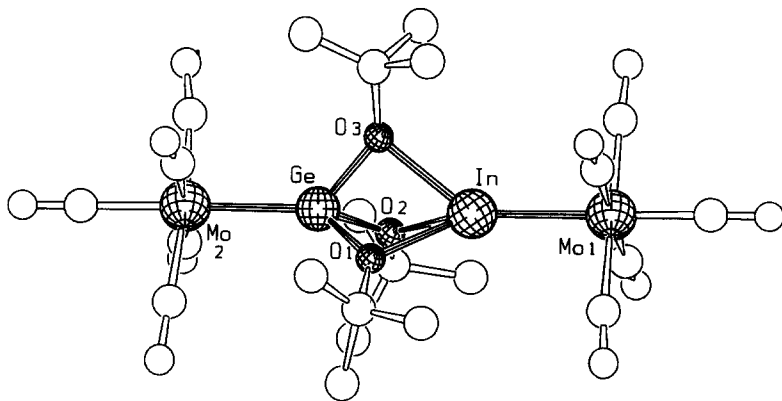


Fig. 3. Molecular structure of  $(\text{CO})_5\text{Mo}-\text{In}(\text{OtBu})_3\text{Ge}-\text{Mo}(\text{CO})_5$  (**MIGM**).

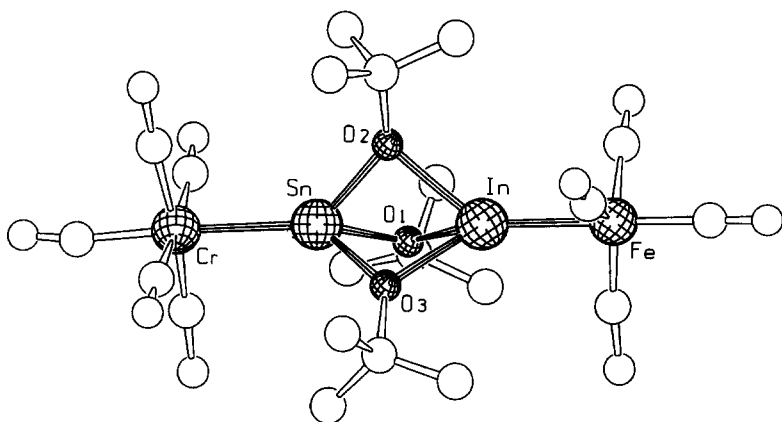


Fig. 4. Molecular structure of  $(\text{CO})_4\text{Fe}-\text{In}(\text{OtBu})_3\text{Sn}-\text{Cr}(\text{CO})_5$  (**FISC**).

Sn(II) with Ge(II) or Pb(II) in mixed metal alkoxides [9]. The difference in structures between **GICIG** and **TSMST** may therefore be attributed to steric factors. The factors responsible for cis or trans arrangements in metal carbonyl complexes may be equilibrated in **CSIMISC**. In this case only, both cis and trans isomers can be detected by NMR in solution. This suggests that in some instances crystal packing or solubility may also play an important role.

Generally, the metal–metal distance in the trigonal bipyramidal cages  $\text{M}'(\text{O}^t\text{Bu})_3\text{M}$  and  $\text{M}'(\text{O}^t\text{Bu})_3\text{M}(\text{O}^t\text{Bu})_3\text{M}'$  along the threefold axis is decreased when transition metals coordinate to the  $ns^2$  elements (Table 5). At the same time, the  $\text{M}'-\text{O}$  distances decrease. The drain of electron density from the main group metal to the transition metal is reflected by a shrinkage of the radius of the metallic atom. This generalization is valid for In(I) and Ge(II) in any of the compounds under discussion and also for Sn(II), with some restrictions, as can be seen by comparing

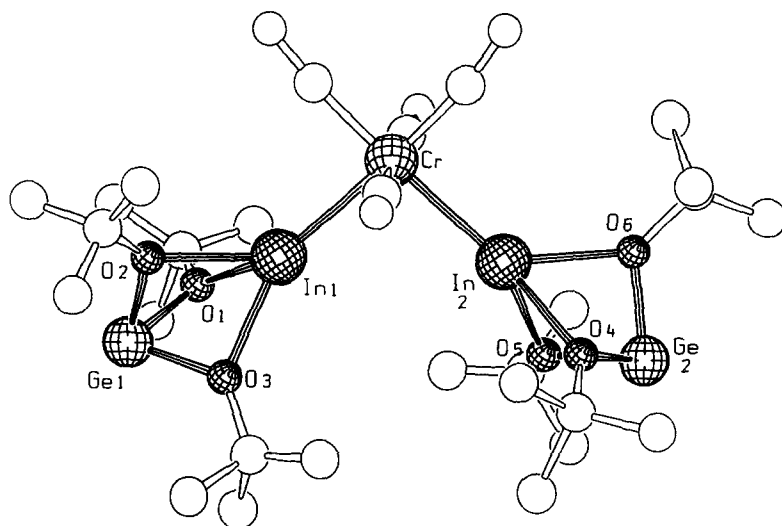


Fig. 5. Molecular structure of  $\text{Ge}(\text{OtBu})_3\text{In}-\text{Cr}(\text{CO})_4-\text{In}(\text{OtBu})_3\text{Ge}$  (**GICIG**).

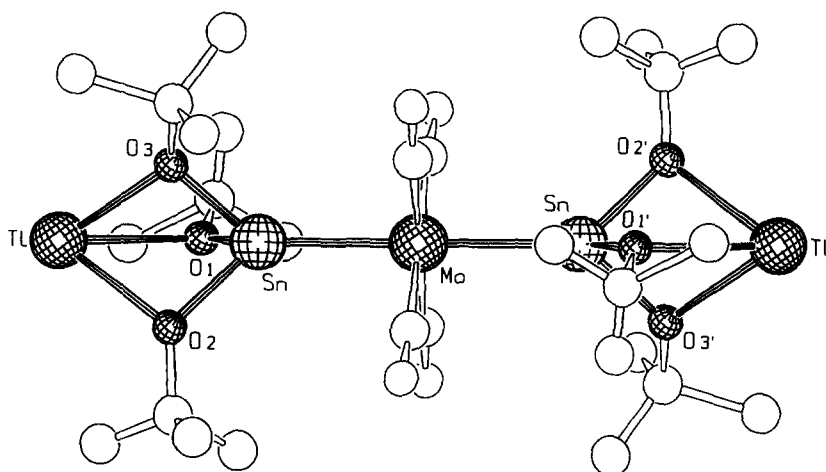


Fig. 6. Molecular structure of  $\text{Tl}(\text{OtBu})_3\text{Sn}-\text{Mo}(\text{CO})_4-\text{Sn}(\text{OtBu})_3\text{Tl}$  (**TSMST**).

the distances in  $\text{Tl}(\text{O}^t\text{Bu})_3\text{Sn}$  (**TS**) with  $\text{Tl}(\text{O}^t\text{Bu})_3\text{Sn}-\text{Mo}(\text{CO})_5$  (**TSM**). However, there are also some exceptions. For example, the Sn–O distances in **MISC** and **MISM** are longer than in the parent compound  $\text{Sn}(\text{O}^t\text{Bu})_3\text{In}$  (see Table 5). To gain further understanding about this effect, we have selected some data from Table 5 and Fig. 2 and rearranged them in Fig. 10. All the compounds in Fig. 10 contain the bipyramid  $\text{In}(\text{O}^t\text{Bu})_3\text{Sn}$ . The smallest distance between indium and tin is obtained in **FISC** and increases within the series **MISM**, **MISC**, **CSICISC**, **CSIMISC**. It can therefore be concluded that the coordination of iron and chromium at indium and

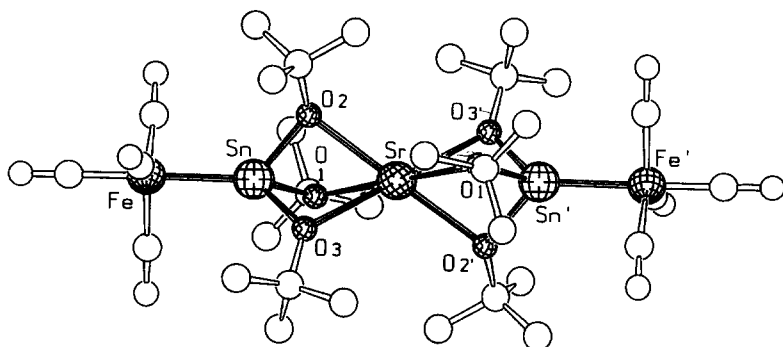


Fig. 7. Molecular structure of  $(\text{CO})_4\text{Fe-Sn}(\text{OtBu})_3\text{Sr}(\text{OtBu})_3\text{Sn-Fe}(\text{CO})_4$  (FSSSF).

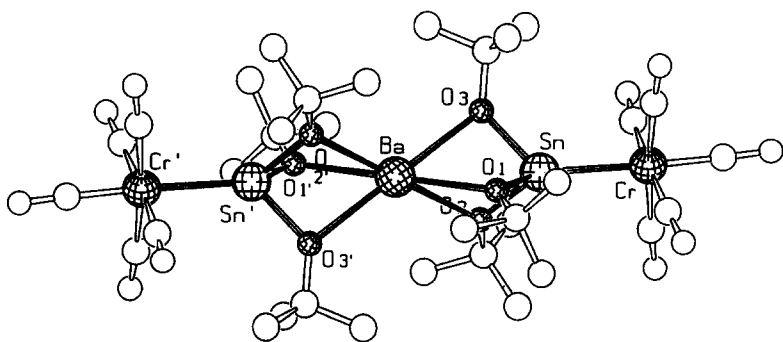


Fig. 8. Molecular structure of  $(\text{CO})_5\text{Cr-Sn}(\text{OtBu})_3\text{Ba}(\text{OtBu})_3\text{Sn-Cr}(\text{CO})_5$  (CSBSC).

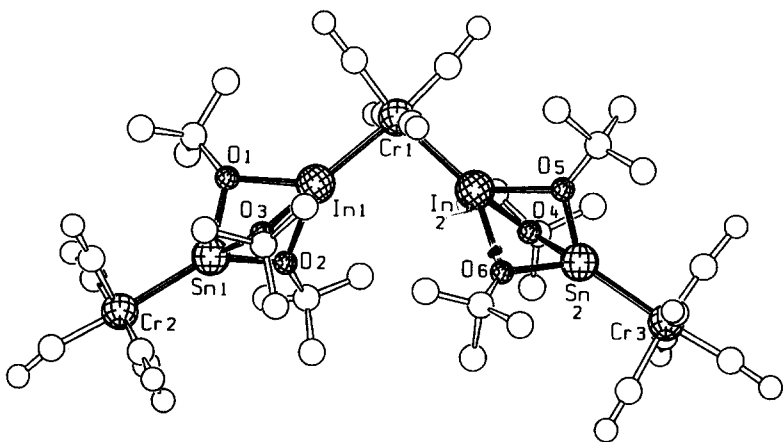


Fig. 9. Molecular structure of  $(\text{CO})_5\text{Cr-Sn}(\text{OtBu})_3\text{In-Cr}(\text{CO})_4\text{-In}(\text{OtBu})_3\text{Sn-Cr}(\text{CO})_5$  (CSICISC). The compound CSIMISC is isotopic to CSICISC (see also Table 4).

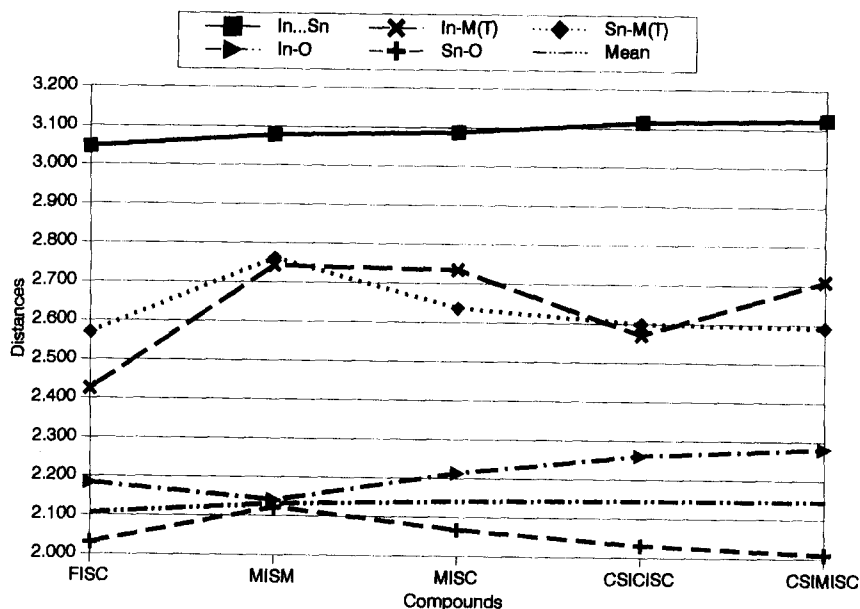


Fig. 10. Compounds containing  $\text{In}(\text{OtBu})_3\text{Sn}$  as metal alkoxide. The distances are given in Å.

tin, respectively, is most effective with respect to the drain of electrons from the main group metals to the transition elements. The metal combinations Mo–Mo or Mo–Cr are less powerful than the combination Fe–Cr. In addition, the radii shrinkage is much more important at indium than germanium and tin, as can be concluded from the In–O distances in the metal carbonyl complexes compared with the free molecule  $\text{In}(\text{O}^t\text{Bu})_3\text{Sn}$ . The mean shrinkage of the In–O distances is about 8% and that of the Ge–O distances is 2.5%. In complexes which contain only tin as the  $ns^2$  element (FSSSF, FSPSF, CSBSC) the shrinkage is even less (0.6%). This parallels our findings with respect to reactivity (see above), i.e.  $\text{In}(\text{I}) \gg \text{Ge}(\text{II}) > \text{Sn}(\text{II})$ .

Inspection of Table 5 and Fig. 10 shows that the two  $ns^2$  elements In(I) and Sn(II) are not isolated from one another. The average of the In–O and Sn–O distances for each compound parallels the In  $\cdots$  Sn distance (Fig. 10). On the other hand, the Sn–O distance may even increase with respect to  $\text{In}(\text{O}^t\text{Bu})_3\text{Sn}$  (in MISM and MISC), but this increase is compensated for by an even higher shrinkage at the In site. These observations clearly show that the  $\text{In}(\text{O}^t\text{Bu})_3\text{Sn}$  part of the molecule is highly flexible and cage expansions on one side are followed by contractions on the other side and vice versa. Partial charge transfer within the cage may be conducted via the trigonal planar oxygen atoms or direct metal  $\cdots$  metal interactions.

In Fig. 11 only those complexes with chromium bonded to tin are included. The Cr–Sn distance within this series is constant, and the plot indicates that the most important contribution to the Sn  $\cdots$  M distances comes from the metal atom (In, Ba) that is incorporated in the alkoxide cage. Thus the M–O and Sn  $\cdots$  M

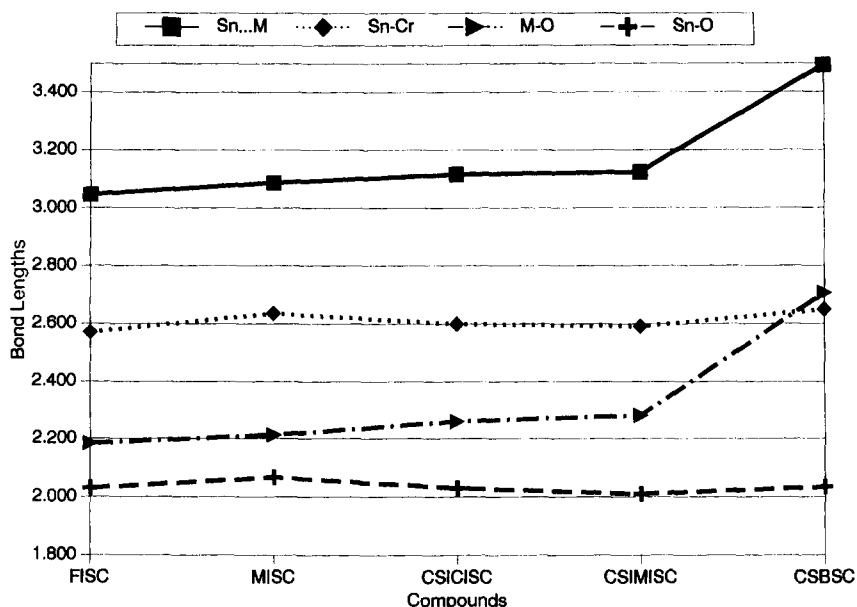


Fig. 11. Compounds with Sn–Cr bonds. The bond lengths are given in Å. The Sn···M curve and the M···O curve are almost parallel to one another.

curves are almost parallel to each other. As expected (Fig. 11), a transition metal atom coordinated to one  $\text{In}(\text{O}^t\text{Bu})_3\text{Sn}$  unit has a more important electron-attracting effect than the same transition metal with two  $\text{In}(\text{O}^t\text{Bu})_3\text{Sn}$  cages attached (**MISC** versus **CSIMISC**).

Compounds of the spirocyclic system  $(^t\text{BuO})\text{M}'(\text{O}^t\text{Bu})_2\text{M}(\text{O}^t\text{Bu})_2\text{M}(\text{O}^t\text{Bu})_2\text{M}'(\text{O}^t\text{Bu})$  can also be used as precursors for metal carbonyl complexes [13]. The iron carbonyl complex  $(\text{CO})_4\text{Fe}-\text{Sn}[\text{O}^t\text{Bu}](\text{O}^t\text{Bu})_2\text{Co}(\text{O}^t\text{Bu})_2\text{Co}(\text{O}^t\text{Bu})_2-[\text{O}^t\text{Bu}]\text{Sn}-\text{Fe}(\text{CO})_4$  has been characterized by X-ray crystallography. As in the compounds discussed above, the coordination of the iron carbonyl to the tin atom results in a decrease in the Sn–O bond length and the Sn···Co distance. Altogether six metallic elements are combined in the molecule in a one-dimensional fashion with an Fe–Sn···Co angle of  $140.1^\circ$  [13].

### 3.2. IR frequencies of CO in metal carbonyl complexes of mixed metal alkoxides

The  $A_1$  resonance in the IR spectra of substituted metal carbonyls of the type  $\text{M}(\text{O}^t\text{Bu})_3\text{M}'-\text{M}^T(\text{CO})_n$ ,  $\text{M}^T(\text{CO})_n-\text{M}(\text{O}^t\text{Bu})_3\text{M}'-\text{M}^T(\text{CO})_n$ ,  $\text{M}(\text{O}^t\text{Bu})_3\text{M}'-\text{M}^T(\text{CO})_n\text{M}'(\text{O}^t\text{Bu})_3\text{M}$  or  $(\text{CO})_n\text{M}^T-\text{M}'(\text{O}^t\text{Bu})_3\text{M}(\text{O}^t\text{Bu})_3\text{M}'-\text{M}^T(\text{CO})_n$  may be used as a probe to distinguish between different substitution patterns in the “Janus-Head” molecules. Figure 12 shows that there are distinct regions in which the  $\nu\text{CO}$  stretch appears for CO trans to the  $\text{M}'-\text{M}^T$  bond. As we have noted before, the C=O stretch

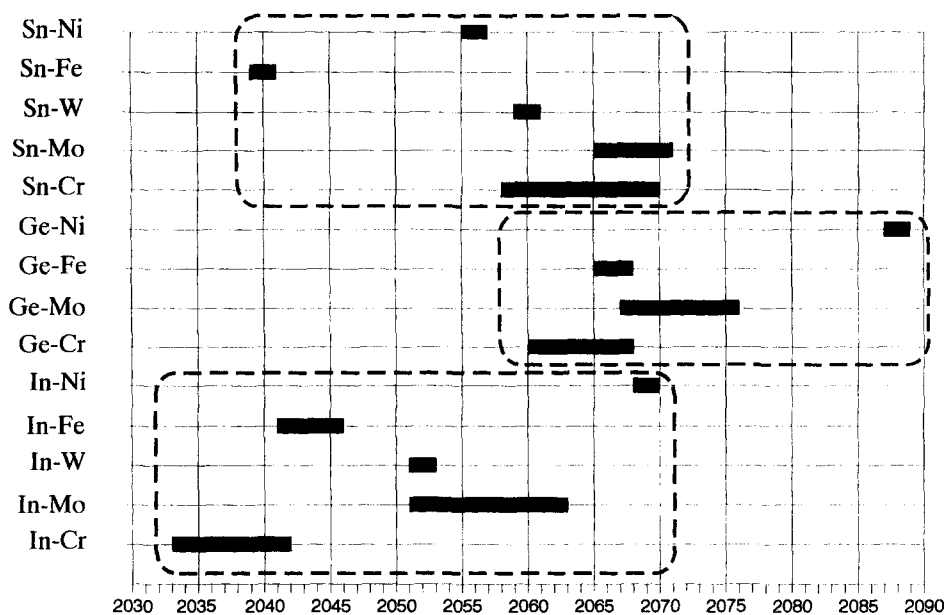


Fig. 12. CO absorption regions (wavenumbers,  $\text{cm}^{-1}$ ) of carbonyl groups trans to the metal-metal bonds indicated in the graph.

may be used as a probe of the extent of  $\pi$ -bonding to the metal carbonyl complex of mixed metal alkoxides. We would expect a shift to higher frequencies compared with standard THF complexes [23] for CO groups trans to the  $M'-M^T$ -bond if there is an important  $M' \leftarrow M^T$  back-bonding via  $\pi$ -orbitals. From a consideration of the trans-carbonyl stretching frequencies in Table 3 it is clear that back-bonding from  $M^T$  to  $M'$  is present. All complexes with  $ns^2$ -metal donors seem to be reasonably strong  $\sigma$ -donors and weak to moderate  $\pi$ -acceptors. This can be concluded from the fact that alkylphosphine-substituted metal carbonyls have comparable wavenumbers [34,35]. Nevertheless, there are some interesting cases to be discussed in more detail. In Fig. 13 several compounds with similar substitution patterns have been assembled. Comparing the data for **SIC** and **SIM**, it is clear that an In-Mo bond should have more  $\pi$ -interaction than an In-Cr bond as the wavenumber of the latter  $A_1$  CO vibration is  $28 \text{ cm}^{-1}$  less [neglecting the different experimental conditions (see Table 3)]. This effect is again observed (of the same magnitude) if **GIC** is compared with **GIM**. We therefore conclude that an In-Mo interaction is stronger than an In-Cr interaction. This interpretation finds its equivalent in molecular dimensions (see Fig. 2), in that all bonds adjacent to indium are much more effected by Mo coordination than by Cr coordination.

When the bidentate "Janus-Head" molecules **MISC**, **MISM**, **MIGC** and **MIGM** are compared with the monodentate species **SIC**, **SIM**, **GIC** and **GIM**, the resonance peaks of the CO vibrations trans to the In-Mo bond are shifted to lower

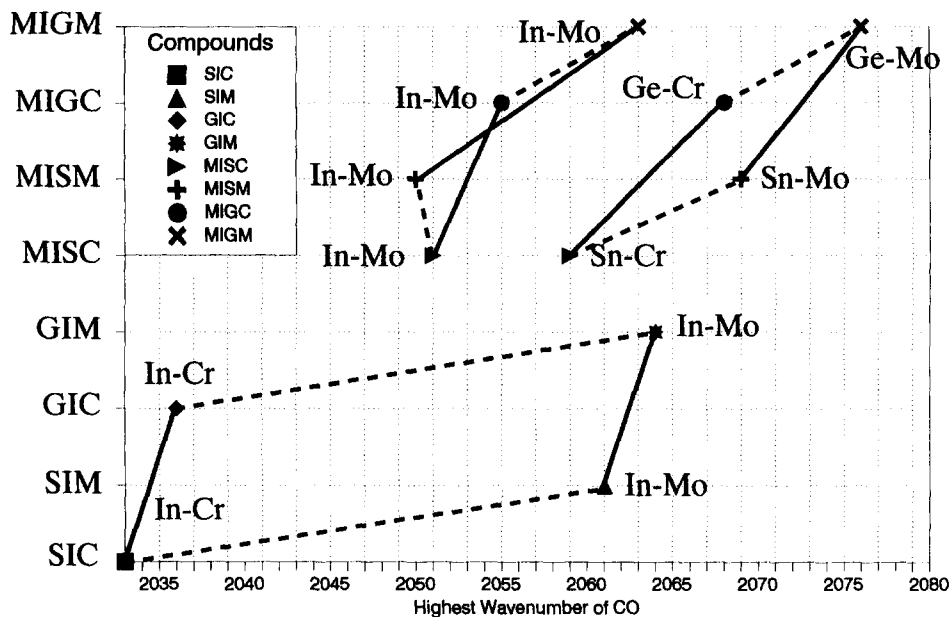


Fig. 13. Stretching frequencies (wavenumbers,  $\text{cm}^{-1}$ ) of the CO absorption trans to the indicated metal-metal bonds in compounds of the families  $\text{Sn}(\text{O}^i\text{Bu})_3\text{In}-\text{M}^{\text{T}}(\text{CO})_5$  ( $\text{M}^{\text{T}} = \text{Cr}, \text{Mo}$ ) and  $(\text{CO})_5\text{Mo}-\text{In}(\text{O}^i\text{Bu})_3\text{Sn}-\text{M}^{\text{T}}(\text{CO})_5$  ( $\text{M}^{\text{T}} = \text{Cr}, \text{Mo}$ ).

wavenumber (with exception of **MIGM**). This means that the second transition metal ligand entering the molecule at the Ge or Sn end has an impact also on the In–Mo bond. Again this is in accordance with our observation in the last section that bond lengths are affected by a second transition metal coordination at parts of the molecule which are not directly linked to the coordination centre. For the germanium or tin end of the molecules **MISC**, **MISM**, **MIGC** and **MIGM**, the CO groups at molybdenum again show higher wavenumbers than the CO groups attached to chromium, but the difference is much less than in the indium case. Also, the wavenumbers for CO trans to Sn–Cr or Sn–Mo are smaller than those which are trans to Ge–Cr and Ge–Mo, respectively, indicating a more important  $\pi$ -backbonding at germanium than tin. With respect to the transition metals we may note that molybdenum results in stronger bonds to indium than chromium. As can be seen from Fig. 14, there is a dependence between the shift of the  $\text{CO}(A_1)$  trans to the Cr–Sn bond and the  $\text{Sn} \cdots \text{In}$  distance. Interestingly the highest CO stretch is found for the shortest  $\text{Sn} \cdots \text{In}$  distance. Again, this may be taken as a criterion for an electron transfer along the metal–metal axis (directly or indirectly through the oxygen bridges of the alcoholate ligand). No correlation can be found for a similar plot of the Sn–Cr distance versus the CO stretching frequency.

A qualitative MO model may be used to explain the different mesomeric effects in the carbonyl IR absorption of mixed metal alkoxide metal carbonyl complexes.

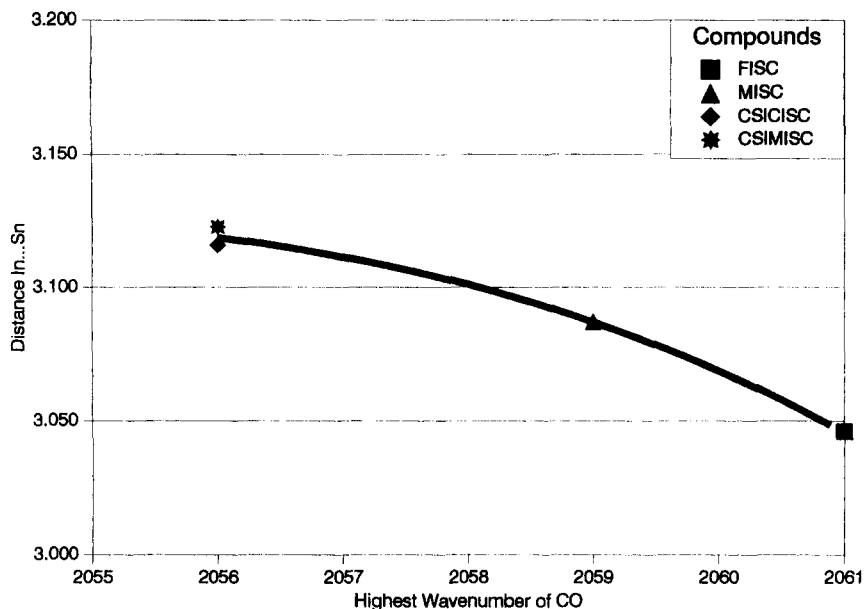


Fig. 14. Correlation of the  $\nu(\text{CO}) A_1$  band ( $\text{cm}^{-1}$ ) with In...Sn distance (Å) in selected compounds.

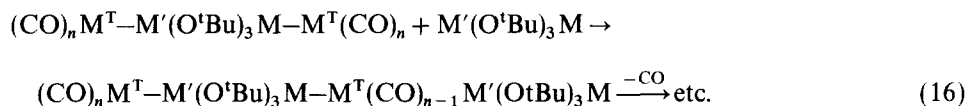
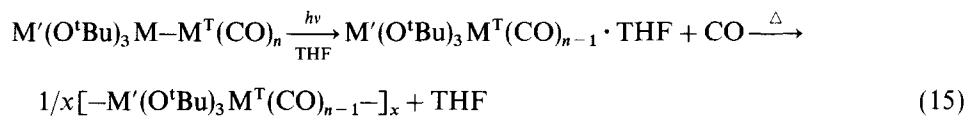
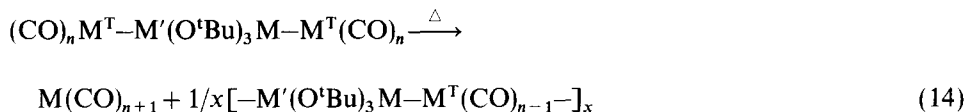
As the d-orbitals of the main group metals are high in energy compared with the d-orbitals of the transition metals,  $\sigma^*$ -orbitals of the mixed metal alkoxides must also be considered for back-bonding from the transition metal to the main group metal. The model would suggest an increase in length of the  $M'-O$  bonds when  $\pi$  back-bonding is taking place through  $\sigma^*$ -orbitals, and no change in the  $M'-O$  distances when  $\pi$ -bonding is occurring through d-orbitals of the main group metals. As can be deduced from the experimental results, in many cases the inductive effects are dominant. In any case, Mo should be more appropriate than Cr for  $\pi$ -bonding as the energy levels of the 4d orbitals match better the orbitals of In(I) and Sn(II), in agreement with the experiment (see above).

### 3.3. Comments on a cluster concept

So far we have considered the distance between metal atoms bridged by alkoxo groups as predominantly non-bonding. This fits in with the observation that all transition metal complexes of the  $ns^2$ -configured metal alkoxides described above are colourless and may be classified as insulators. Nevertheless, a detailed look at the molecular dimensions (see above) reveals that the main group metals under consideration are very close to each other. Moreover, there are direct metal-metal bonds between the transition metals and the  $ns^2$  elements. The one-dimensional metal chain therefore consists of di- or triatomic metal clusters separated by oxygen bridges. Within the metal chain the metallic elements are tightly linked or in loose



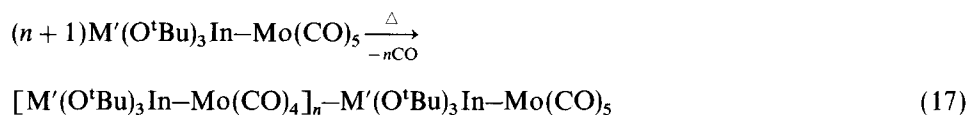
atoms. Theoretically, there are several promising reaction pathways to obtain oligomers or polymers of the type  $[M'(O^tBu)_3M-M^T(CO)_n]_x$ , some of which are displayed in reactions (14)–(16).



Unfortunately, none of these reactions give the desired products; instead, equilibria of mono-  $[(CO)_nM^T-M(OtBu)_3M']$  and dicoordinated alkoxides  $[(CO)_nM^T-M'(O^tBu)_3M-M^T(CO)_n]$  are obtained. If the temperatures are raised too high rapid degradation of the starting materials is observed.

Switching from  $M(O^tBu)_3M'$  to the system  $M'(O^tBu)_3M(O^tBu)_3M'$  does not improve the results (with respect to the formation of oligomers). Nevertheless, when  $Sn(O^tBu)_3Sr(O^tBu)_3Sn$  reacts with norbornadiene chromium tetracarbonyl, an insoluble yellow powder is obtained which shows one IR absorption in the CO region ( $1880\text{ cm}^{-1}$ ). From the analytical data this product seems to be a mixture of  $Sn(O^tBu)_3Sr(O^tBu)_3Sn-Cr(CO)_4-Sn(O^tBu)_3Sr(O^tBu)_3Sn$  and  $[Sn(O^tBu)_3Sr(O^tBu)_3Sn-Cr(CO)_4]_x$ . Unfortunately, we have not yet been able to separate these compounds.

Very recently we have been successful in the synthesis of the first oligomeric metal carbonyl–metal alkoxide systems [eqn. (17)].



$M' = \text{Ge, Sn}$

The two starting materials **GIM** and **SIM** behave slightly differently. Upon thermolysis of **GIM** in refluxing xylene the product precipitates, whereas the thermolysis of **SIM** works best in the melt at about  $135^\circ\text{C}$ . An insoluble product is again obtained which deposits from the melt.

The oligomer obtained from **SIM** has been extensively studied. Its IR spectrum contains three major bands in the carbonyl stretching region [ $2012 (A_1^{1b})$ ,  $1940$

( $A_1^{1a}$ ), 1891 ( $B_1$ )]. All bands are shifted to lower wavenumbers compared with **SIM** (Table 3), which is an indication of a second coordination of a main group metal at the molybdenum centres. Further the difference in the high-frequency  $A_1$  band between **SIM** and its oligomer ( $\Delta\nu$  49  $\text{cm}^{-1}$ ) is typical for the transition from mono- to disubstitution, as may be concluded from the pairs of complexes  $(\text{CO})_5\text{Mo}[\text{MeP}(\text{OMe})_2]$  versus  $(\text{CO})_4\text{Mo}[\text{MeP}(\text{OMe})_2]_2$  ( $\Delta\nu = 47 \text{ cm}^{-1}$ ) [38],  $(\text{CO})_5\text{Mo}(\text{AsPh}_3)$  versus  $(\text{CO})_4\text{Mo}(\text{AsPh}_3)_2$  ( $\Delta\nu = 51 \text{ cm}^{-1}$ ) [39] and  $(\text{CO})_5\text{Mo}(\text{AsEt}_3)$  versus  $(\text{CO})_4\text{Mo}(\text{AsEt}_3)_2$  ( $\Delta\nu = 55 \text{ cm}^{-1}$ ) [40]. In addition, the  $ns^2$  element substituents are (at least to a significant extent) in a cis arrangement as determined from the IR absorption patterns. A partial trans arrangement cannot be excluded, however, since the single absorption band of the trans isomer (local symmetry  $D_{4h}$ ) would be in the same region as the strong  $B_1$  band of the cis isomer (local symmetry  $C_{2v}$ ). There is a tiny absorption shoulder at  $2055 \text{ cm}^{-1}$ , which we attribute to the trans-CO stretch in an  $\text{Mo}(\text{CO})_5$  group (compare **MISM** or **MISC**). This may be indicative of a terminal group and therefore it seems reasonable to assume that the product is not a cyclic oligomer but a chain oligomer. From the intensity ratio of the  $A_1$  band at  $2012 \text{ cm}^{-1}$  and the shoulder at  $2055 \text{ cm}^{-1}$ , a rough estimation may be made of the number of units  $n$  in  $[\text{Sn}(\text{O}^t\text{Bu})_3\text{In}-\text{Mo}(\text{CO})_4]_n$   $\text{Sn}(\text{O}^t\text{Bu})_3\text{In}-\text{Mo}(\text{CO})_5$ , which should be about 10.

In addition to the analytical data, which are in accord with the oligomer, the quantitative gas evolution has been studied by gas volumetry and by mass spectrometry and unambiguously shows the only gas being evolved during the reaction to be carbon monoxide. The volumetry results in 85–90% CO evolution starting with the pure compound **SIM**. Taking this number into account, a ratio  $\text{Mo}(\text{CO})_4$  to  $\text{Mo}(\text{CO})_5$  of 9:1 in the product is calculated, which is in accord with the result from IR spectroscopy. Thus the chain length should be  $n=9$  or 10 in  $[\text{Sn}(\text{O}^t\text{Bu})_3\text{In}-\text{Mo}(\text{CO})_4]_n$   $\text{Sn}(\text{O}^t\text{Bu})_3\text{In}-\text{Mo}(\text{CO})_5$ .

We have not yet determined if the product is uniform or if there is a mixture of several different oligomeric species. The immediate precipitation from the melt indicates that the degree of oligomerization does not vary very much. Unfortunately, we were not able to record a  $^{119}\text{Sn}$  MAS (magic angle spinning) NMR spectrum of the solid, as the molybdenum isotope  $^{97}\text{Mo}$  has a high quadrupole moment. On the other hand, this even seems to confirm that Sn is indeed bound to Mo. The  $^{13}\text{C}$  CP (cross-polarization) MAS NMR spectrum is fairly simple with resonances at 34.7, 76.8, 205 and 209 ppm and is different from that of the starting compound **SIM** (35.8, 70.4, 200 and 203 ppm in benzene solution). Interestingly, the resonances for the CO groups are shifted to higher  $\delta$ -values, which is again indicative of a second substitution at molybdenum [41]. The signals of the *tert*-butyl groups are sharp (indicative of a uniform product), whereas the resonance signals for the carbonyls are broad and overlapping. Unfortunately, they cannot be resolved in order to distinguish the CO end-group [for experimental reasons (signal-to-noise ratio and relaxation time), the  $^{13}\text{C}$  CP-MAS NMR techniques give better results than the

MAS experiment, especially in the CO resonance region]. The oligomers obtained from eqn. (17) are pale yellow and darken on contact with air. So far no physical measurements on cooperative effects along these one-dimensional, “percolated” metal rows have been performed.

#### ACKNOWLEDGEMENTS

We thank the Fonds der Chemischen Industrie and the Deutsche Forschungsgemeinschaft for financial support.

#### REFERENCES

- 1 M. Petz, Chem. Rev., 86 (1986) 1019.
- 2 M. Veith, Angew. Chem., 99 (1987) 1; Angew. Chem., Int. Ed. Engl., 26 (1987) 1.
- 3 M. Veith, Phosphorus Sulfur Silica, 41 (1989) 195.
- 4 M. Veith, Chem. Rev., 90 (1990) 3.
- 5 *Janus*, Roman god with two faces; *January* is the month pointing in two opposite directions: one to the old year, the other to the new year; in the “Janus-Head” molecules the metallic elements are situated on opposite faces of the O<sub>3</sub> triangle.
- 6 R.C. Mehrotra, Adv. Inorg. Chem. Radiochem., 26 (1983) 269.
- 7 D.C. Bradley, Chem. Rev., 89 (1989) 1317.
- 8 K.C. Caulton and L.G. Hubert-Pfalzgraf, Chem. Rev., 90 (1990) 969.
- 9 M. Veith, J. Hans, L. Stahl, P. May, V. Huch and A. Sebal, Z. Naturforsch., Teil B, 46 (1991) 403.
- 10 M. Veith and R. Rösler, Angew. Chem., 94 (1982) 867; Angew. Chem., Int. Ed. Engl., 21 (1982) 858.
- 11 M. Veith and K. Kunze, Angew. Chem., 103 (1991) 92; Angew. Chem., Int. Ed. Engl., 30 (1991) 95.
- 12 M. Veith and R. Rösler, Z. Naturforsch., Teil B, 41 (1986) 1071.
- 13 M. Veith, D. Käfer, J. Koch, P. May, L. Stahl and V. Huch, Chem. Ber., 125 (1992) 1033.
- 14 W. Strohmeier and K. Gerlach, Chem. Ber., 94 (1961) 398.
- 15 W. Strohmeier, Angew. Chem., 76 (1964) 873; Angew. Chem., Int. Ed. Engl., 3 (1964) 730.
- 16 M. Grenz and W.W. du Mont, J. Organomet. Chem., 241 (1983) C5.
- 17 M. Grenz, E. Hahn, W.W. du Mont and J. Pickardt, Angew. Chem., 96 (1984) 69; Angew. Chem., Int. Ed. Engl., 23 (1984) 61.
- 18 P.B. Hitchcock, M.F. Lappert, S.A. Thomas and A.J. Thorne, J. Organomet. Chem., 315 (1986) 27.
- 19 M.A. Bennett, L. Pratt and G. Wilkinson, J. Chem. Soc., (1961) 2037.
- 20 E.W. Abel and F.G.A. Stone, Q. Rev. Chem. Soc., 24 (1970) 498.
- 21 F.A. Cotton, Prog. Inorg. Chem., 21 (1976) 1.
- 22 A. Vincent, Molecular Symmetry and Group Theory, Wiley, Chichester, 1977.
- 23 J. Weidlein, U. Müller and K. Dehnicke, Schwingungsspektroskopie, Georg Thieme, Stuttgart, 1982.
- 24 M. Veith, H. Lange, K. Bräuer and R. Bachmann, J. Organomet. Chem., 216 (1981) 377.
- 25 J.D. Cotton, P.J. Davidson and M.F. Lappert, J. Chem. Soc., Dalton Trans., (1976) 2275.
- 26 J.D. Cotton, P.J. Davidson, D.E. Goldberg, M.F. Lappert and K.M. Thomas, J. Chem. Soc., Chem. Commun., (1974) 893.

- 27 D.F. Shriver, P.W. Atkins and C.H. Langford, *Inorganic Chemistry*, Oxford University Press, Oxford, 1990.
- 28 Further details of the crystal structure investigations may be obtained from the Fachinformationszentrum Karlsruhe, Gesellschaft für Wissenschaftliche Information mbH, D-76344 Eggenstein-Leopoldshafen, Germany, on quoting the depository number CSD 58225, the names of the authors and the journal citation.
- 29 M. Veith and J. Hans, *Angew. Chem.*, 103 (1991) 845; *Angew. Chem., Int. Ed. Engl.*, 30 (1991) 878.
- 30 F.A. Cotton and C.S. Kraihanzl, *J. Am. Chem. Soc.*, 84 (1962) 4432.
- 31 J.D. Atwood and T.L. Brown, *J. Am. Chem. Soc.*, 98 (1976) 3160.
- 32 J.K. Burdett, *Inorg. Chem.*, 14 (1975) 375.
- 33 D.L. Lichtenberger and T.L. Brown, *J. Am. Chem. Soc.*, 100 (1978) 366.
- 34 J. Dalton, I. Paul, J.G. Smith and F.G.A. Stone, *J. Chem. Soc. A*, (1968) 1195.
- 35 R.J. Mawby and C. White, *J. Chem. Soc., Chem. Commun.*, (1968) 312.
- 36 M. Veith and K. Kunze, results to be published.
- 37 H. Preut and H.J. Haupt, *Acta Crystallogr., Sect. B*, 35 (1979) 2191.
- 38 G. Bouquet and M. Bigorgne, *Bull. Soc. Chim. Fr.*, (1962) 433.
- 39 C.E. Jones and K.J. Coskran, *Inorg. Chem.*, 10 (1971) 55.
- 40 E.O. Fischer and R.J.J. Schneider, *Chem. Ber.*, 103 (1970) 3684.
- 41 L.J. Todd and J.R. Wilkinson, *J. Organomet. Chem.*, 77 (1974) 1.